IEEE Access
Multidisciplinary | Rapid Review | Open Access Journal

Received March 8, 2020, accepted April 22, 2020, date of publication April 27, 2020, date of current version May 22, 2020.

Digital Object Identifier 10.1109/ACCESS.2020.2990454

Flexible Multi-Energy Scheduling Scheme for Data Center to Facilitate Wind Power Integration

PENG WANG, YUJIE CAO, (Student Member, IEEE), AND ZHAOHAO DING, (Member, IEEE)
School of Electrical and Electronics Engineering, North China Electric Power University, Beijing 102206, China

Corresponding author: Zhaohao Ding (zhaohao.ding@ncepu.edu.cn)

This work was supported in part by the National Key Research and Development Program of China under Grant 2018YFE0196000, in part by the Ministry of Science and Technology of State Grid Corporation of China through a support project under Grant SGBJDK00KJJS1900085, in part by the National Natural Science Foundation of China under Grant 51907063, in part by the Fundamental Research Funds for the Central Universities under Grant 2019MS054, and in part by the Support Program for the Excellent Talents in Beijing City.

ABSTRACT Due to the intermittent and uncontrollable nature of wind resources and inflexible operation of conventional generation units, they present challenges for the power system to integrate more wind power. With its unique flexibility on the demand side, the data center can be considered as an effective solution to relieve wind curtailment. Moreover, with the help of waste heat recovery module, the data center can reduce the utilization of conventional thermal units especially in the residential heating sector which increases the flexibility of system operation and facilitates more renewable integration. In this paper, a flexible workload management and resource scheduling model are proposed to achieve a multi-energy co-optimization for data center and enhance the integration of wind power. A two-stage stochastic programming model is formulated to address the uncertainties involved in this process. The proposed model is examined by a simulative data center microgrid and the numerical results demonstrate its effectiveness and robustness.

INDEX TERMS Data center, workload allocation, wind energy, waste heat recovery, energy management.

I. INTRODUCTION

Although the wind harvesting techniques have been developed greatly, it still presents significant challenges to integrate more wind power into power grid due to its intermittent and uncontrollable nature. It is reported that nearly 17% of wind power generated (more than 50 TWh) was curtailed in China in 2016 [1], [2]. It is simulated that 42 million tons of CO_2 emission can be reduced if the abandoned wind of China was fully utilized [2], [3]. Therefore, exploring the reasons and solutions for facilitating more wind power integration is critical from both economic and environmental perspective.

One of the reasons for wind power curtailment is the mismatch between enormous wind power generation and limited energy demand caused by transmission congestion [3], [4]. It is reported that about 10% of the wind power curtailment is introduced by the capacity limitation of transmission [5]. As stated in [3], the maximum daily fluctuation of wind power can reach 80% of the installed capacity of the utility grid. And the wind power profile depicts a certain anti-peak characteristic. Therefore, an effective solution to improve the integration of wind power is to enhance the flexibility of demand side. Zheng *et al.* stated in [4] that one of the reasons for the rejection of the wind energy is due to the limited power demand and prior dispatched traditional energy. Another reason for wind power curtailment is the inflexibility of the power system operation during residential heating seasons, which have contributed more than 90% of wind power curtailment in Northeast China [5]. This is particularly significant in the cold areas in which centralized residential heating is much needed. The widely used combined heat and power (CHP) units increase inflexibility of the power system since their minimal power outputs are coupled with residential heating needs. Consequently, the capability of integrating wind power to the system would be jeopardized. For instance, the wind curtailment during the residential heating periods in Northeast China in 2015 is 26.94 TWh [5]. Wu *et al.* established analytical models to clarify the causes and mechanisms resulting in high growth and low wind power capacity usage in [6]. As shown in [7], Jafari *et al.* presented an optimization

The associate editor coordinating the review of this manuscript and approving it for publication was Reinaldo Tonkoski.

approach for annual planning of renewable generations and diesel generators, to reduce the cost and ensure the reliability of the microgrid operation.

Besides the academia, many methods and techniques have been analyzed and implemented in industry to solve this severe problem as well. Internet companies have made outstanding contribution therein particularly. Data centers, as the fundamental infrastructure of the cloud computing industry, have experienced a significant increase in both number and size for the last decades. The number of data centers worldwide is estimated to be 8.4 million in 2017 [8] and may remain its growing tendency for the upcoming decades. Global growth in internet penetration and cloud computing paradigms has driven computing service providers, such as Google, Amazon, and Microsoft, focusing on the hyperscale data center construction facilities [9]. At the same time, this industry contributes a considerable part of energy consumption worldwide. It is predicted that data centers will be responsible for more than 30% of global electricity consumption in 2025 [10]. From this point of view, the total operation cost of data center is significantly affected by its energy supply cost. Apart from that, greenhouse gas (GHG) emission is also top-of-mind concerns for the data center operators. Therefore, making data center operation more energy-efficient is becoming a critical undertaking.

As an integrated flexible multi-energy hub, the data center operator needs to optimize interactive resources scheduling decisions to meet the workload requirements [11]. As some of the flexible workloads could be rescheduled after arrived on the servers, they could be shifted from on-peak to off-peak electricity tariff hours, or from light wind periods to strong wind periods if wind resources are available, which gives a great opportunity to deal with the wind curtailment situation in some areas and achieve the maximum economic and environmental benefits for the whole system.

Many researches have paid attention on the performance of IT workload scheduling on energy saving and wind power utilization. Yu *et al.* proposed the energy management framework for data center microgrid with stochastic renewable generation considered in the system in [12], and jointly analyzed the economic and environmental performance of the workload allocation on the overall microgrid operation. Wang *et al.* did similar work on decentralized data centers in [13]. Compared to [12], the authors in [13] applied a different solution by utilizing dual decomposition to solve the problem, and showed different angles of the improved results. Based on that, Guo *et al.* proposed a stochastic programming model for data center microgrids with renewable energies and thermal storage system considered [14]. Kwon *et al.* developed a decision-making model based on two-stage stochastic programming considering servers operation of the data center and power procurement for demand response (DR) [15]. To be specific, the model proposed in it exploited an explicit working algorithm for servers in data center and paid attention on the computation performance of the servers and the cost saving of the procedure, without regard to the overall operation of the system. Kim *et al.* explored the impact of placement for data centers for the purpose of wind curtailment reduction and cost savings [16].

In the meantime, data center is reported to be a promising role in providing heat to the residential heating sector. It is convinced that almost all the electricity that information technology (IT) servers, which are instrumental equipment in data centers, consumed is converted into heat [17]. Managing the thermal circumstance of the computing room is essential for data center. Therefore, reusing the waste heat dissipated from the numerous IT servers could remove the redundant heat and repurpose it in heating one's own premises. This attracts a growing attention in both academia and industry [18]–[21]. As the cases in [19] depicted, the data centers in Nordic countries have several benefits, including cold climate, cheap rent and electricity, high share of renewables penetration, etc. Finnish district heating utilities have estimated data centers as the second most potential source for waste heat, after the forest industry.

To the best of our knowledge, even though numbers of research works have been done on power management of data centers for cost saving, environmental footprint reduction and energy efficiency improvement, limited literature has considered the heat and power co-optimization potentials within a data center microgrid, especially on the perspective of facilitating wind power integration. The unique multi-energy operation characteristics of data center can positively contribute to integrating more wind power. On the one hand, the optimally scheduled shift-able batch workload can re-shape the electricity load profile to better coordinate with the wind generation profile. On the other hand, with the help of the waste heat recovery (WHR) module, data center microgrid can reduce the requirement of heating supply from conventional CHP units, which increases the flexibility of the power system operation and capability of integrating more wind power. Therefore, both economic and environmental benefit can be achieved by optimally scheduling multi-energy resources in the data center microgrid.

This paper proposes a flexible multi-energy scheduling scheme to manage the resources from both supply and demand sides of a data center microgrid. The objective is to reduce wind power curtailment and minimize operation cost while both heat and power resources scheduling are considered. The proposed model is formulated as a two-stage stochastic programming problem to address the uncertain characteristics of wind power and energy demand [22]–[26]. According to the listed researches, the first stage variables should be determined prior to others, and the second stage variables should be scheduled later. In this paper, the first stage is defined as day-ahead scheduling stage. The hourly scheduling decisions are optimized in the first stage with deterministic forecasting results to minimize the operation cost and greenhouse gas (GHG) emission for the data center microgrid. In the second stage which is defined as real-time balancing stage, the decisions from the first stage are adjusted to satisfy the constraints associated with different scenarios.

TABLE 1. List of symbols.

Sets and indices:			
T	Index set of time intervals. $t \epsilon T$	U	Index set of CHP generation units. $u \in U \& U \in I$
S	Index set of scenarios. $s \epsilon S$	I	Index set of all kinds of generation units. $i \in I$
V	Index set of power-only generation units. $v \in V \& V \in I$	W	Index set of heat-only generation units. $w \in W \& W \in I$
Deterministic Parameters:			
π_e	Average external cost for GHG emissions.	M	Number of servers in the data center
L_C	Number of workload capacity in the data center	α	Coefficient factor of the CHP unit
$P_{grid,max}$	Transmission line capacity	$\pi_{grid}(t)$	Spot price in the electric wholesale market at time *t*.
κ	Coefficient factor in the waste heat recovery module	$R_u(i)$,$R_d(i)$	Ramp-up and ramp-down limit for generation unit *i*
$\vartheta_g(t)$	Coefficient factor of GHG emission from the utility grid at time t	$\vartheta_{gen}(i,t)$	Coefficient factor of GHG emission from the generator *i* at time *t*
a(i),b(i),c(i)	Coefficient factor of the operation cost of the generator *i*.	$P_{gen,max}$, $P_{gen,min}$	Power output limitation for generation unit i
$H_{gen,max}$, $H_{gen,min}$	Thermal output limitation for generation unit i		
Stochastic Parameters:			
$P_{wd}(t,s)$	Wind power output at time *t* in scenario *s*	$L_{ds}(t,s)$	Delay-sensitive workloads at time *t* in scenario *s*
$Q_{thm}(t,s)$	Heating demands in district heating area at time *t* in scenario *s*		
Decision Variables:			
$P_{gen}(i,t)$	Power produced by generation unit *i* at time *t*	$H_{gen}(i,t)$	Heat produced by generation unit *i* at time *t*
$L(t)$	Processing workload at time *t*	$\sigma_{load}(t)$	Processed workload at time *t*
$L_{dt}(t)$	Delay-tolerant workload arrived to the data center at time *t*	$P_{dc}(t,s)$	Power consumed by the data center at time *t* in scenario *s*
$H_{dc}(t,s)$	Heat recovered from the data center at time *t* in scenario *s*	$P_{grid}(t)$	Power bought by the utility grid at time *t*
$P_{chp}(u,t)$	Power produced by CHP generation unit *u* at time *t*	$H_{chp}(u,t)$	Heat produced by CHP generation unit *u* at time *t*
$P_p(v,t)$	Power produced by power-only generation unit v at time t	$H_h(w,t)$	Heat produced by heat-only generation unit *w* at time *t*
$Q_L^{dt}(t)$	Cumulative quantity of the delay-tolerant workloads till time *t*	$r_{gen}^{e,U}(i,t,s)$, $r_{gen}^{e,D}(i,t,s)$	Upward and downward adjustment on the heat generation of generation unit *i* at time *t* in scenario *s*
$r_{gen}^{h,U}(i,t,s)$, $r_{gen}^{h,D}(i,t,s)$	Upward and downward adjustment on the heat generation of generation unit *i* at time *t* in scenario *s*	$r_{chp}^{e,U}(u,t,s)$, $r_{chp}^{e,D}(u,t,s)$	Upward and downward adjustment on the power generation of CHP unit *u* at time *t* in scenario *s*
$r_{grid}^{U}(t,s)$, $r_{grid}^{D}(t,s)$	Increase and decrease of the amount of power purchased from the utility grid at time *t* in scenario *s*	$r_{chp}^{h,U}(u,t,s)$, $r_{chp}^{h,D}(u,t,s)$	Upward and downward adjustment on the heat generation of CHP unit *u* at time *t* in scenario *s*

In this way, the optimal multi-energy scheduling scheme for data center can be achieved under the stochastic environment.

Compared with existing works, the contributions of this paper are summarized into 3 parts:

1. The flexible IT workload allocation decisions are co-optimized with other resource scheduling decisions to minimize the operation cost of data center microgrid and enhance wind power integration.
2. Data center workload allocation (DCWA) and the WHR decisions are optimized simultaneously in the proposed flexible multi-energy scheduling scheme. With the WHR module as linkage between thermal and the power system, the optimally allocated workloads could benefit the demand side of the power system and supply side of thermal system simultaneously.
3. The optimal multi-energy scheduling scheme is analyzed to demonstrate the benefits of DCWA and the WHR on both economic and environmental perspectives. Numerical test cases with four different configurations are examined to illustrate their impacts respectively.

The remaining of this paper is arranged as follows. Section 2 depicts the model framework of the proposed model. The mathematical formulations are established in Section 3. Section 4 provides numerical test cases to illustrate the effectiveness of the proposed model and evaluates its economic, environmental impacts. The conclusion is present in Section 5.

II. MODEL DESCRIPTION

The definition of data center microgrid should be clear at first. As is known to all, data center needs tremendous amount of stable power supply, and the data center operator business is investment-intensive and economies of scale dominate as

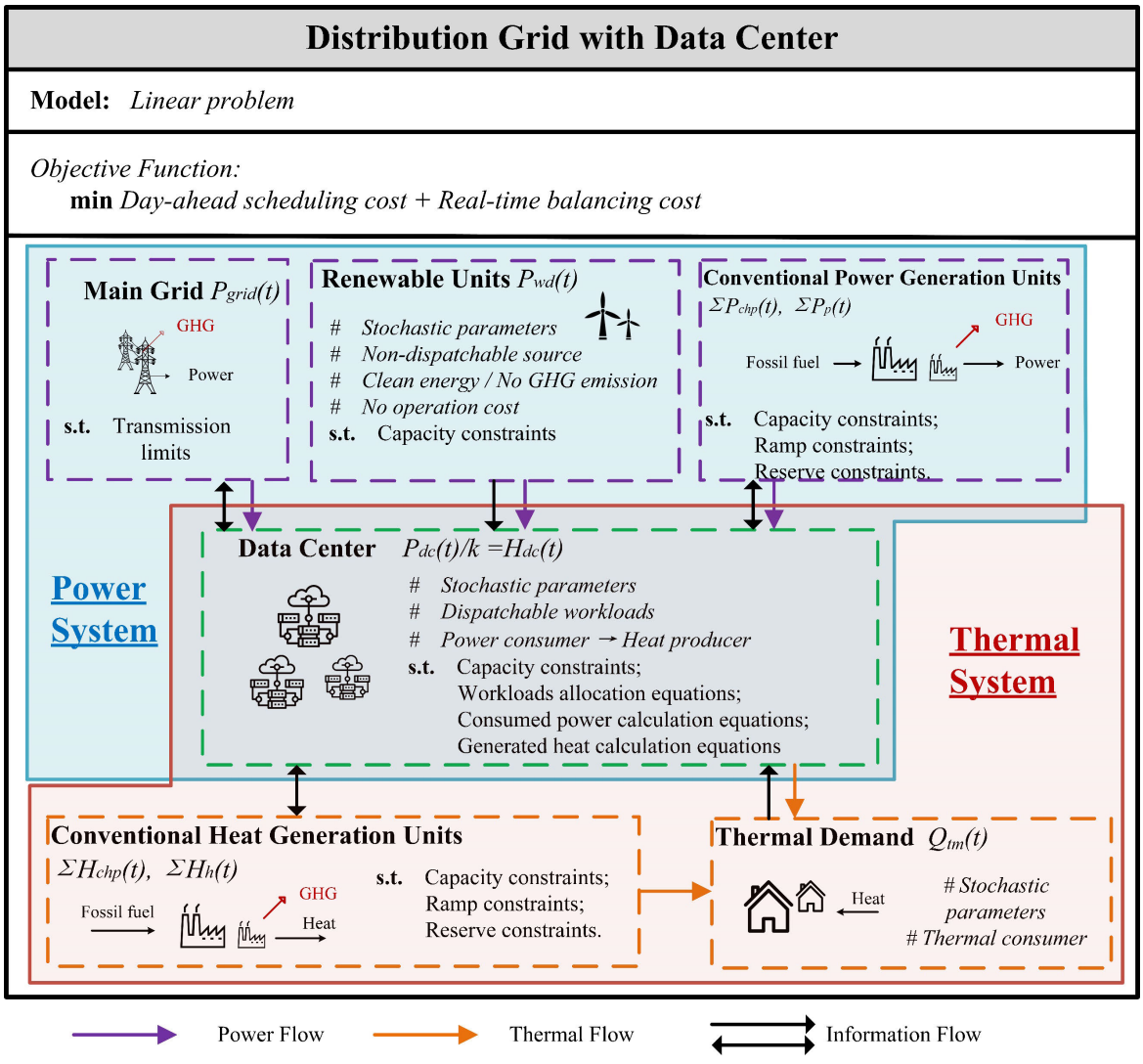

FIGURE 1. Architecture of the proposed system.

a generic business strategy [19]. Thus, a data center industry generally equips several supplementary energy suppliers except the utility grid, such as conventional generation units, renewable generation units, etc. Therefore, data center could be operated on-site or off-site. In this monopoly system, data center has been placed into the position where it has ability to acquire the construction and operation data of the generators and schedule the resources. As a result, the 'data center-centric' power supply system is considered as a data center microgrid [27]–[29].

The architecture of the proposed model for a data center microgrid is shown in Fig. 1. It can be observed that the power sector is equipped with resources such as on-site conventional power generators (PGs, i.e. CHP units and power-only units), distributed renewable units (i.e. wind turbines), and procurement from utility grid. And the data center could be considered as the power consumer. In the thermal sector, the proposed model includes heat resources such as the WHR module from the data center, and on-site heat generators (HGs, i.e. CHP units and heat-only units). And the residential heating area is the heat consumer as well. As shown in Fig. 1, the power system and thermal system are coupled via the WHR module for data center.

The workloads of data center can be classified into delay-sensitive workloads and delay-tolerant workloads. Delay-sensitive workloads generally refer to the service requests that must be processed within a very short time, usually a few seconds. With the inelastic processing time, quality of service (QoS) is required to maintain agreed when serving this kind of computational jobs [30]. With homogeneous servers, the arrival time of the delay-sensitive workloads are usually modelled as Poisson distribution during the operating day of the data center [13]. On the contrary, delay-tolerant workloads, such as cloud computing tasks, are more flexible with the execution duration time. This kind of workloads are computational-intense jobs that are not

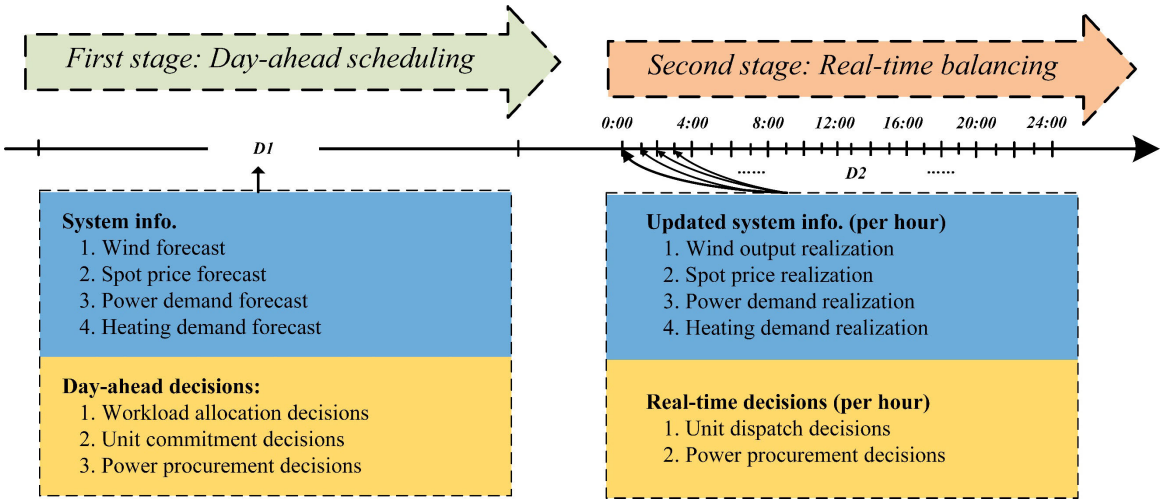

FIGURE 2. Architecture of the proposed programming.

expected to be processed immediately. In other words, they could be re-allocated to another time slot as long as it is within the given completion deadline thus QoS can be guaranteed. The duration time could range from minutes to hours [11], [31].

In the proposed model, the decision portfolios for DCWA and resource scheduling are achieved in a two-stage framework, as shown in Fig. 2. Meanwhile, the spot price of electric wholesale market, outputs of wind power generation and energy demand are considered as stochastic parameters. A two-stage stochastic programming formulation is adopted to address those uncertainties. For the first stage, the operation cost, which includes unit commitment cost, power procurement cost and emission cost, is optimized in day-ahead manner. In contrast to that, the second stage decision making is the adjustment decisions in real-time in response to the random realization of stochastic parameters [32]. The objective of proposed model is designed to maximize the economic and environmental benefit of the target system. Therefore, both operation cost and GHG emission are considered in the objective function. Since the WHR module works as the linkage of the thermal and power system, the allocation decisions for delay-tolerant workloads would not only affect the operation of the power system as a demand but also affect the operation of thermal system as a potential source. Consequently, the power system and thermal system in a data center microgrid can be coordinated by optimally managing the shift-able DCWA along with other resources.

Combined all the aforementioned factors together, a combined heat and power co-optimization model for optimal DCWA and resources scheduling is proposed for a data center microgrid. Both economic and environmental impacts are included in the objective function and a two-stage stochastic programming approach is adopted to address the uncertainty in this process.

III. COMPONENT MODELS AND MATHEMATICAL FORMULATIONS

A. OBJECTIVE FUNCTION

As stated above, the proposed model aims to minimize the operation cost and GHG emission within the data center microgrid by optimally allocating the delay-tolerant workload and scheduling generation resources. Therefore, this model could be modelled as a multi-objective problem. In this study, monetization of the environmental impacts has been applied in the objective function [33], which could overcome the limitation of subjective weighting factors assignment.

A two-stage stochastic programming technique [22]–[24] is adopted by this model to address the uncertainties in this proposed problem. The generic mathematical formulation of the proposed model is shown in (1). The uncertainty nature of the independent stochastic parameters is characterized by the probability distribution of their day-ahead forecasting errors, which are considered as normal distribution [34]. To characterize their uncertain characteristics, a large number of scenarios are generated through Monte Carlo (MC) approach to represent the probability distributions of those stochastic vectors [35], [36]. In the proposed model, Latin Hypercube Sampling (LHS) method is applied to reduce the number of scenarios [37].

$$\min\ C = \{\Phi(x) + E[\Theta(x,\xi)]\} \tag{1}$$

$$s.t.\ H(x,\xi) = 0 \tag{2}$$

$$G(x,\xi) \geq 0 \tag{3}$$

$$\xi = [P_{wd}, L_{ds}, Q_{thm}] \tag{4}$$

In the above formulation, $\Phi(x)$ represents the operation cost in the day-ahead dispatch model, which is considered as objective function of the first-stage problem, and $\Theta(x,\xi)$ represents the cost in the real-time balancing model, which is considered as objective function of the second-stage problem. In these formulations, x represents the vector of decision

variables, which in this model are continuous variables with time scale discretization. The continuous variables comprise of the scheduling decisions for generation outputs and power procurement in day-ahead dispatch model and real-time balancing model. The $H(x,\xi)=0$ and $G(x,\xi)\geq 0$ represent the constraints of this model. In (4), ξ is the uncertainty set including the output of wind resources, which is defined as P_{wd}, delay-sensitive workloads for the data center, which are defined as L_{ds}, and heating demands in the district heating area, which is defined as Q_{thm}.

It should be noted that the deviation between the day-ahead information and real-time information is the forecasting error. And the uncertainty level of the stochastic parameters is measured by the variance of forecasting error [35]. Considering the adjustment function in the second stage, the proposed stochastic optimization model would minimize the operation cost and GHG emission cost and the expected value of adjustment in the operating stage simultaneously over the entire operation time span. In this way, a flexible multi-energy scheduling model for the target data center microgrid can be achieved.

1) DAY-AHEAD SCHEDULING COST

In this paper, the power supply cost and emission cost are considered as deterministic parameters. The objective formulation in the day-ahead scheduling stage is shown in (5). As it illustrates, the first-stage objective refers to the cost of power supply, which includes the operation cost of all fossil-fuel generators (including all the power generators and heat generators), denoted as F_{gen}, and power purchase cost, denoted as F_{grid}, and GHG emission cost $\mathrm{F_{GHG}}$ [38].

For the simplicity, the operation cost of on-site generation units is linearized as stated in [37], [39]. $\pi_{grid}(t)$ is the spot price in the electric wholesale market at time t. $\vartheta_g(t)$ and $\vartheta_{gen}(i,t)$ are the emission factors of external grid and generation unit i at time t, which estimate GHG emissions from various sources of air pollution. π_e is the average external cost for GHG emissions to quantify the corresponding environmental impact.

$$\begin{aligned}\Phi(x) &= F_{gen}+F_{grid}+F_{GHG}\\ &= \sum\nolimits_t\Big\{\sum\nolimits_i\left[a(i)+b(i)\cdot P_{gen}(i,t)+c(i)\cdot H_{gen}(i,t)\right]\\ &\quad +\pi_{grid}(t)\cdot P_{grid}(t)\\ &\quad +\pi_e\left[\vartheta_g(t)\cdot P_{grid}(t)+\sum\nolimits_i\vartheta_{gen}(i,t)\cdot P_{gen}(i,t)\right]\Big\}\end{aligned} \tag{5}$$

2) REAL-TIME BALANCING COST

As mentioned above, the second-stage objective, as illustrated in (6), is the minimal value of the cost due to the adjustment in the real-time operation stage associated with different realization of uncertainty parameters caused by the forecasting error. To simulate the stochastic characteristics of these uncertainties, stochastic scenarios are simulated by MC approach based on the historical data portfolio, and then S scenarios which follow the distribution of the original datasets are extracted from them by LHS techniques to reduce the randomness. After applying these techniques, the expected value of (6) could be replaced by the average value of all the selected scenarios [36], [40] as shown in (7).

Thus, the objective function of the original two-stage stochastic programming problem could be replaced by a single-stage deterministic formulation as shown in (8) [41].

$$\begin{aligned}\Theta(x,\xi) = \min \sum\nolimits_t\Big\{&\sum\nolimits_i\Big[b(i)\cdot\left(r^{e,U}_{gen}(i,t)-r^{e,D}_{gen}(i,t)\right)\\ &+c(i)\cdot\left(r^{h,U}_{gen}(i,t)-r^{h,D}_{gen}(i,t)\right)\Big]\\ &+\pi_{grid}(t)\cdot\left(r^{U}_{grid}(t)-r^{D}_{grid}(t)\right)\\ &+\pi_e\Big[\vartheta_g(t)\cdot\left(r^{U}_{grid}(t)-r^{D}_{grid}(t)\right)\\ &+\sum\nolimits_i\vartheta_{gen}(i,t)\cdot\left(r^{U}_{gen}(i,t)-r^{D}_{gen}(i,t)\right)\Big]\Big\}\\ &,\forall i,t\end{aligned} \tag{6}$$

$$\begin{aligned}\Theta(x,s) =\frac{1}{S}\sum\nolimits_s\sum\nolimits_t\Big\{&\sum\nolimits_i\Big[b(i)\cdot\left(r^{e,U}_{gen}(i,t,s)-r^{e,D}_{gen}(i,t,s)\right)\\ &+c(i)\cdot\left(r^{h,U}_{gen}(i,t,s)-r^{h,D}_{gen}(i,t,s)\right)\Big]\\ &+\pi_{grid}(t)\cdot\left(r^{U}_{grid}(t,s)-r^{D}_{grid}(t,s)\right)\\ &+\pi_e\Big[\vartheta_g(t)\cdot\left(r^{U}_{grid}(t,s)-r^{D}_{grid}(t,s)\right)\Big]\\ &+\sum\nolimits_i\vartheta_{gen}(i,t)\cdot\left(r^{U}_{gen}(i,t,s)-r^{D}_{gen}(i,t,s)\right)\Big]\Big\}\\ &,\forall i,t,s\end{aligned} \tag{7}$$

$$\begin{aligned}\min C &= \Phi(x)+\Theta(x,s)\\ &= \sum\nolimits_t\Big\{\sum\nolimits_i\left[a(i)+b(i)\cdot P_{gen}(i,t)\right.\\ &\quad\left.+c(i)\cdot H_{gen}(i,t)\right]\\ &\quad+\pi_{grid}(t)\cdot P_{grid}(t)\\ &\quad+\pi_e\left[\vartheta_g(t)\cdot P_{grid}(t)\right.\\ &\quad\left.+\sum\nolimits_i\vartheta_{gen}(i,t)\cdot P_{gen}(i,t)\right]\Big\}\\ &\quad+\frac{1}{S}\sum\nolimits_s\sum\nolimits_t\Big\{\sum\nolimits_i\left[(b(i)+c(i))\right.\\ &\quad\left.\cdot\left(r^{U}_{gen}(i,t,s)-r^{D}_{gen}(i,t,s)\right)\right]\\ &\quad+\pi_{grid}(t)\cdot\left(r^{U}_{grid}(t,s)-r^{D}_{grid}(t,s)\right)\\ &\quad+\pi_e\Big[\vartheta_g(t)\cdot\left(r^{U}_{grid}(t,s)-r^{D}_{grid}(t,s)\right)\\ &\quad+\sum\nolimits_i\vartheta_{gen}(i,t)\cdot\left(r^{U}_{gen}(i,t,s)-r^{D}_{gen}(i,t,s)\right)\Big]\Big\}\\ &\quad,\forall i,t,s\end{aligned} \tag{8}$$

s.t. Day-ahead scheduling equations and constraints (9)-(22)
Real-time balancing equations and constraints (23)-(31)

The constraints in the proposed model can be divided into two types. The first type of constraints are day-ahead scheduling constraints, where the scheduling decisions for unit commitment and utility power procurement are made. The second type of constraints are real-time balancing constraints, where

the generators and energy purchase decisions should be adjusted based on different stochastic parameter realizations.

B. DAY-AHEAD SCHEDULING CONSTRAINTS

1) DATA CENTER CONSTRAINTS

a: WORKLOAD ALLOCATION MODEL

Suppose that there are M identical servers in the data center, the probability of assignments in each server is equal to $1/M$. All the workloads must not exceed the computational limits, which is formulated as (9). L_C represents the number of overall data center workloads due to the CPU limits. And the total workloads at time t consist of delay-sensitive workloads and delay-tolerant workloads minus the processing workloads, as defined in (10), All of the delay-tolerant workloads should enqueue in a FIFO queue during the shifting process, which is shown in (11) [42]. To satisfy the QoS requirements, all of the delayed responses should be executed before the end of its due time, as demonstrated in (12) [18].

$$L(t) \leq L_C, \forall t \tag{9}$$

$$L(t) = L_{ds}(t) + L_{dt}(t) - \sigma_{load}(t), \forall t \tag{10}$$

$$Q_L^{dt}(t) = Q_L^{dt}(t-1) + L_{dt}(t) - \sigma_{load}(t), \forall t \tag{11}$$

$$Q_L^{dt}(T) = 0 \tag{12}$$

b: POWER CONSUMPTION MODEL

In a typical data center, the consumed electricity is concisely divided into two categories based on its consumers, which are IT equipment electricity consumption and non-IT equipment electricity consumption. For the electrical usage awareness, a wide-spread benchmark metric, power usage effectiveness (PUE), is applied to estimate the total power usage based on the two classes of power use, which is defined as a ratio of total power usage to the IT equipment power usage [43]. Thus, the overall power use of the data center could be estimated by (13) as detailed in [44]. In this formulation, $\delta \triangleq P_{idle} + (PUE - 1) P_{peak}$, $\mu \triangleq P_{peak} - P_{idle}$, thereinto P_{idle} and P_{peak} are the minimum and maximum power consumption of each server.

$$P_{dc}(t) = M(\delta + \mu L(t)), \forall t \tag{13}$$

c: HEAT RECOVERY UNIT MODEL

Equation (14) is the function for the WHR module in data center to illustrate the percentage of waste heat can be repurposed for district heating. In the formulation, the WHR conversion factor κ is introduced to represent the efficiency of the WHR module [45].

$$H_{dc}(t) = \kappa P_{dc}(t), \forall t \tag{14}$$

2) GENERATION CONSTRAINTS

For each generation unit, the power and heat production are constrained by the maximum and minimum power output limits, as listed in (15) and (16). The ramping rate constraints for on-site generation units are shown in (17) and (18). Note that power production of HGs is constrained as 0 and the heat production of PGs is constrained as 0 as well. And CHP units should satisfy both power constraints and heating constraints simultaneously. The coupled correlation of heat and power characteristics for CHP unit is model in (19), where α represents the coupled correlation factor of heat and power production for CHP units.

$$P_{gen,min}(i) \leq P_{gen}(i,t) \leq P_{gen,max}(i), \forall i, t \tag{15}$$

$$H_{gen,min}(i) \leq H_{gen}(i,t) \leq H_{gen,max}(i), \forall i, t \tag{16}$$

$$-R_d(i) \leq P_{gen}(i,t) - P_{gen}(i,t-1) \leq R_u(i), \forall i, t \tag{17}$$

$$-R_d(i) \leq H_{gen}(i,t) - H_{gen}(i,t-1) \leq R_u(i), \forall i, t \tag{18}$$

$$P_{chp}(u,t) = \alpha H_{chp}(u,t), \forall u, t \tag{19}$$

3) SYSTEM CONSTRAINTS

a: POWER BALANCE

$$P_{grid}(t) + \sum\nolimits_u P_{chp}(u,t) + \sum\nolimits_v P_p(v,t) + P_{wd}(t) = P_{dc}(t), \forall u, v, t \tag{20}$$

The operation scheduling process must ensure the balance between supply and demand, as shown in (20). The resources are modelled on the left-hand side and the demands are listed on the right-hand side.

b: HEAT BALANCE

$$H_{dc}(t) + \sum\nolimits_u H_{chp}(u,t) + \sum\nolimits_w H_h(w,t) = Q_{thm}(t), \forall u, w, t \tag{21}$$

Similar to the power balance constraint, thermal supply-demand balancing is modelled as (21).

c: POWER PURCHASE CAPABILITY LIMITATIONS

$$P_{grid}(t) \leq P_{grid,max} \forall t \tag{22}$$

Transmission capacity indicates that how much power could be purchased from the utility grid to the distribution grid without compromising system security. So, the power bought from the wholesale market cannot be greater than that capacity, denoted by $P_{grid,max}$, as shown in (22).

C. STOCHASTIC AND REAL-TIME BALANCING MODEL

1) DATA CENTER CONSTRAINTS

a: GENERATION CONSTRAINTS

With the consideration of the upward and downward output adjustment of the on-site generation units, (23) and (24) enforce the generation limitation in day-ahead stage and adjustment limitation in the real-time stage, including power generators and heat generators. Constraint (25) shows the coupled correlation of heat and power production for CHP units considering the adjustment in the real-time balancing stage. In (23)-(25), the upward and downward adjustment

are set as positive and negative decision variables mathematically.

$$P_{gen,min}(i) \le P_{gen}(i,t) + r^{e,U}_{gen}(i,t,s) - r^{e,D}_{gen}(i,t,s) \le P_{gen,max}(i), \forall i,t,s \quad (23)$$

$$H_{gen,min}(i) \le H_{gen}(i,t) + r^{h,U}_{gen}(i,t,s) - r^{h,D}_{gen}(i,t,s) \le H_{gen,max}(i), \forall i,t,s \quad (24)$$

$$P_{chp}(u,t) + r^{e,U}_{chp}(u,t,s) - r^{e,D}_{chp}(u,t,s) = \alpha\left(H_{chp}(u,t) + r^{h,U}_{chp}(u,t,s) - r^{h,D}_{chp}(u,t,s)\right), \forall u,t,s \quad (25)$$

b: REAL-TIME RAMPING CONSTRAINTS

Constraints (26) and (27) illustrate the upward and downward ramping limitations of the adjustment on the on-site generation units in the real-time stage. $r^{e,U}_{gen}(i,t,s)$ and $r^{e,D}_{gen}(i,t,s)$ represent the upward and downward adjustment in scenario s on electricity generation units respectively, and $r^{h,U}_{gen}(i,t,s)$ and $r^{h,D}_{gen}(i,t,s)$ represent the upward and downward adjustment in scenario s on heat generation units accordingly.

$$-R_d(i) \le \left(P_{gen}(i,t) + r^{e,U}_{gen}(i,t,s) - r^{e,D}_{gen}(i,t,s)\right) - \left(P_{gen}(i,t-1) + r^{e,U}_{gen}(i,t-1,s) - r^{e,D}_{gen}(i,t-1,s)\right) \le R_u(i), \forall i,t,s \quad (26)$$

$$-R_d(i) \le \left(H_{gen}(i,t) + r^{h,U}_{gen}(i,t,s) - r^{h,D}_{gen}(i,t,s)\right) - \left(H_{gen}(i,t-1) + r^{h,U}_{gen}(i,t-1,s) - r^{h,D}_{gen}(i,t-1,s)\right) \le R_u(i), \forall i,t,s \quad (27)$$

2) SYSTEM CONSTRAINTS IN REAL-TIME STAGE

The balancing in power and thermal system considering the adjusted power and thermal output relative to the scheduling in day-ahead stage are formulated in (28) and (29). Constraint (30) imposes the power purchase capacity in the real-time stage considering the incremental or lessened changes relative to the scheduling stage. Eq. (31) defines the power consumed by the data center considering the uncertain delay-sensitive workloads and the total workload processing at time t.

$$\left(P_{grid}(t) + r^{U}_{grid}(t,s) - r^{D}_{grid}(t,s)\right) + \sum_u \left(P_{chp}(u,t) + r^{e,U}_{chp}(u,t,s) - r^{e,D}_{chp}(u,t,s)\right) + \sum_v \left(P_p(v,t) + r^{e,U}_{p}(v,t,s) - r^{e,D}_{p}(v,t,s)\right) + P_{wd}(t,s) = P_{dc}(t,s), \forall u,v,t,s \quad (28)$$

$$H_{dc}(t,s) + \sum_u \left(H_{chp}(u,t) + r^{h,U}_{chp}(u,t,s) - r^{h,U}_{chp}(u,t,s)\right) + \sum_v \left(H_h(w,t) + r^{h,U}_{h}(w,t,s) - r^{h,U}_{h}(w,t,s)\right) = Q_{thm}(t,s), \forall u,w,t,s \quad (29)$$

$$P_{grid}(t) + r^{U}_{grid}(t,s) - r^{D}_{grid}(t,s) \le P_{grid,max}, \forall t,s \quad (30)$$

$$P_{dc}(t,s) = M\left[\delta + \mu \cdot \left(L_{ds}(t,s) + L_{dt}(t) - \sigma_{load}(t)\right)\right] \forall t,s \quad (31)$$

IV. CASE STUDY

A. SYSTEM CONFIGURATION

1) SETUP DATA

In this section, the proposed model is examined with real-world data to evaluate the performance. Table 2 reports the major technical parameters of data center and other key components. Table 3 lists the economic parameters of those on-site generation units. In this paper, the ratio of delay-sensitive workloads and delay-tolerant workloads for data center is assumed as 50:50 while in practice the workloads percentage of those two categories varies depending on targeting customers [46]. Three conventional generation units, which are CHP unit, power-only unit, and heat-only unit, are included in the data center microgrid as controllable generation resources. The CHP unit and heat-only unit are fuelled by natural gas and power-only unit is coal-fuelled.

TABLE 2. Technical parameters of data center, on-site generation units, and transmission line limits.

Facility	Parameters	Values	Source
Data center	Number of IT servers	11.25×10^5	[55]
	Max power consumption (MW)	225	
	Maximum power allowance for server rack (W)	200	
	No-loaded power consumption for server rack (W)	100	[27]
	PUE	1.2	
	κ (WHR conversion factor)	70%	[20, 45]
Grid tie	Maximum grid procurement capability (MW)	120	-
On-site generation units	α (Coupled correlation factor for CHP unit)	1.1	[56]
	Initial output of CHP, power-only unit and heat-only unit (MW)	0, 0, 0	
	Max power/heat output limit of CHP, power-only unit and heat-only unit (MW)	55, 50, 120	
	Min power/heat output limit of CHP, power-only unit and heat-only unit (MW)	6, 0, 10	
	Ramping up/down rate of CHP, power-only unit and heat-only unit (MW/h)	5, 4, 8	
	Upward/downward reserve of CHP, power-only unit and heat-only unit (MW)	10, 5, 11	

In this paper, IT workloads of data center, heating demand, and wind power output are assumed as stochastic parameters. The stochastic parameters are considered as independent parameters. Hourly data for Nov. 28th, 2018 of every parameters is collected from several sources. The reason for choosing this day is that the temperature on that day is low and the heat demand in the system is high, which could make the inflexibility of the system caused by power and thermal generation constraints more prominent. The workload data is

TABLE 3. Economic parameters of on-site generation units.

Parameters		Value	Source
Startup and shutdown cost of CHP, power-only unit and heat-only unit ($)		250, 300, 200	[39]
Operation cost factors	a(i) of CHP, power-only unit and heat-only unit ($)	82.5, 35.10, 50.22	
	b(i) of CHP, power-only unit and heat-only unit ($/MW)	37.14, 95.18, 0	
	c(i) of CHP, power-only unit and heat-only unit ($/MW)	6.73, 0, 61.5	

derived from IT workload forecaster in [31]. And the delay-tolerant workloads are assumed to be executed within a day.

The spot price data is obtained from PJM wholesale market, as shown in Fig. 3(1). The wind speed data are obtained from [47], and the wind power outputs are calculated based on [48], as shown in Fig. 3(2). The correlation of spot price dataset and wind power dataset is calculated to be −0.597, which means that they have negative impact on the other. As shown in Fig. 3(1) and Fig. 3(2), the spot price climbs during 0:00 to 12:00 and achieve the maximum value at 12:00, while the wind power profile decreases and reach the minimum at 15:00. Then during 12:00 to 24:00, the spot price decreases and the wind power profile climbs.

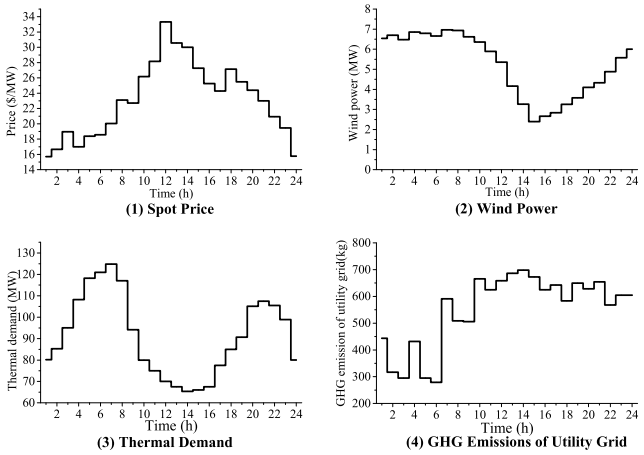

FIGURE 3. Hourly historical values of spot price, wind power, heating demand and GHG emission of the utility grid.

And the thermal requirement is considered as residential heating demand, which varies with temperature. As reported in Fig. 3(3), heating demand is generated based on historical temperature data in Pennsylvania, USA, assisted by the algorithm demonstrated in [49]. What's more, as described above, the waste heat generated from the data center could not be utilized by the heating demand with long distance transmission and low-grade recaptured heat. In the reality, some data centers industries choose to equip other energy conversion facilities, such as boilers, to heat up and make good use of the waste heat for district heating. Some technologies are striking to develop the insulation of the district heating network, which could feed the lower-grade heat to the residential heating requirement [19].

As the primary GHG emitted through human activities [50], CO_2 emission is considered in the proposed model to evaluate the environmental implication. The emission parameter of on-site generation units and external cost of CO_2 are reported in Table 4 based on [51], [52]. And the hourly emission factor of the utility grid is calculated by the historical marginal unit mix data of PJM [53]. The calculation method is shown in [54]. As is known, generators connected to the utility grid use different types of fuels, which have different emission accordingly. With the original hourly generation data fuelled by gas, coal etc., and the emission factors shown in Table 5, the hourly GHG emission of the utility grid could be calculated, shown in Fig. 3(4).

TABLE 4. Parameters of the GHG external costs and the emission factors of the gas- and coal-fueled generators.

Emission Type	External Cost ($/kg)	Gas-fuelled Generator (kg/MWh)	Coal-fuelled Generator (kg/MWh)	Source
CO_2	31.48	357	918	[51, 52]

TABLE 5. The performance indexes (CSR, GERR, and WCR) of each configuration.

	CSR (%)	WCR (%)	GERR (%)
CI	23.39	2.77	11.16
CII	12.60	3.08	8.67
CIII	17.80	3.67	2.01
CIV	-	7.96	-

Based on the historical data scenarios of the uncertainties, 1000 scenarios are generated through Monte Carlo simulation. After scenario reduction method, 10 scenarios are remained. The model is then solved by CPLEX 12.0 solver on a computer with AMD X6 CPU@2.70 GHz and 8 GB memory.

2) TEST CASE CONFIGURATION

To illustrate the effectiveness of the proposed workload management and resource scheduling model for data center microgrid, four configurations with different functionalities, as shown in the following, are investigated in this paper.

Configuration I (CI): Optimal case with DCWA and WHR.

Configuration II (CII): Comparison case with DCWA but without WHR.

Configuration III (CIII): Comparison case without DCWA but with WHR.

Configuration IV (CIV): Reference case without both DCWA and WHR.

3) PERFORMANCE INDEXES

To demonstrate the economic and environmental performance of proposed model in different configurations, three performance indexes are introduced as shown in the following.

a: Cost saving ratio (CSR)

CSR, as shown in (32), is defined as the relative cost reduction of the nth configuration compared to the reference case **CIV**. In this equation, C_4 is the total operation cost of **CIV** and C_n is that of the nth configuration proposed above. Higher of CSR means lower costs in the system of this configuration.

$$CSR = \frac{(C_4 - C_n)}{C_4} \times 100\% \quad n = 1, 2, 3 \tag{32}$$

b: WIND CURTAILMENT RATIO (WCR)

WCR is defined as the ratio of the actually consumed wind power in the nth configuration to the potential generation capability, as shown in (33). $P_{wd,n}$ and $P_{wd',n}$ are the daily consumed wind power and the predicted data in the nth configuration respectively. Lower WCR means that fewer wind power is curtailed, that is, more wind power utilization in the system of this configuration.

$$WCR = \frac{P_{wd,n}}{P_{wd',n}} \times 100\% \quad n = 1, 2, 3, 4 \tag{33}$$

c: GHG EMISSION REDUCTION RATIO (GERR)

GERR represents the ratio of the GHG emissions reduction compared to the reference configuration to evaluate the environmental performance as defined in (34). $E_{GHG,4}$ and $E_{GHG,n}$ represent the daily GHG emissions in the fourth configuration and nth configuration respectively. Higher GERR means that fewer GHG is emitted in the system of this configuration.

$$GERR = \frac{\left(E_{GHG,4} - E_{GHG,n}\right)}{E_{GHG,4}} \times 100\%, \quad n = 1, 2, 3 \tag{34}$$

B. NUMERICAL RESULTS

1) SETUP DATA

The numerical simulation results of each configuration are reported in Fig. 4 to Fig. 6. The optimal DCWA decisions for those four cases are shown in Fig. 4. Combining Fig. 4 with and Fig. 3, it can be observed that the delay-tolerant workloads in **CI** and **CII** are shifted to the periods with lower electricity price and higher heating demand, such as 0:00 to 8:00 and 21:00 to 24:00 as shown in Fig. 4 (1) and Fig. 4 (2). Moreover, it should be mentioned that the onshore wind resources typically have larger outputs during this time interval [47]. Consequently, the optimally rescheduled workloads in **CI** and **CII**, not only served the heating demand but also enhance wind power integration. Compared to that, the delay-tolerant workloads in **CIII** and **CIV** are non-dispatchable and must be served upon arrival. As shown in Fig. 4(3) and Fig. 4(4), those workloads arrive mainly during the peak hours such as 9:00 to 16:00. Therefore, the benefit of the WHR in those cases would not be fully utilized by the peak heating demand.

Fig. 5 shows the power generation and consumption portfolio of the proposed data center microgrid in four configurations respectively. The histograms above the horizontal axis represent the power generated from wind turbines and PGs,

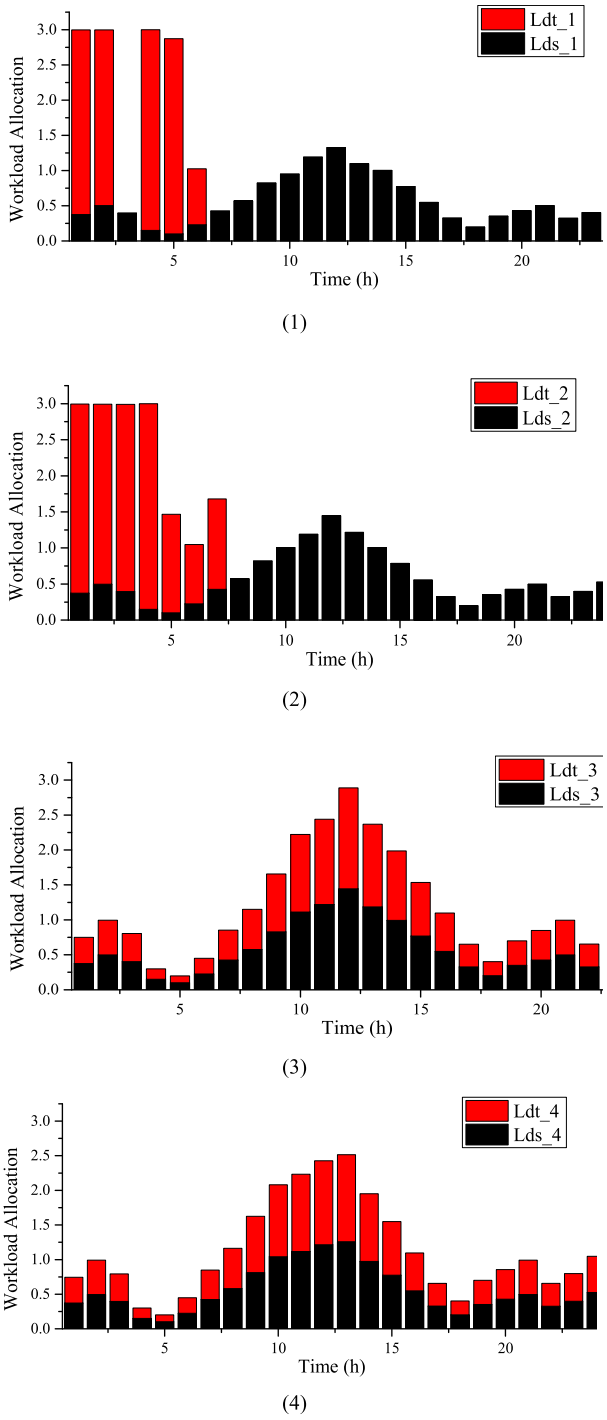

FIGURE 4. Results of DCWA for four configurations.

and purchased from the utility grid. And the power consumption is depicted below the horizontal axis. It can be observed in Fig. 5(1) that most of the electric power comes from the utility grid, especially during the early morning and late night, when the spot market price is relatively low. At the same time, the second highest power generation comes from the CHP unit to meet the peak power and heat requirements simultaneously as shown in Fig. 3 and Fig. 5(1). Furthermore, on-site wind resources contribute during all day especially

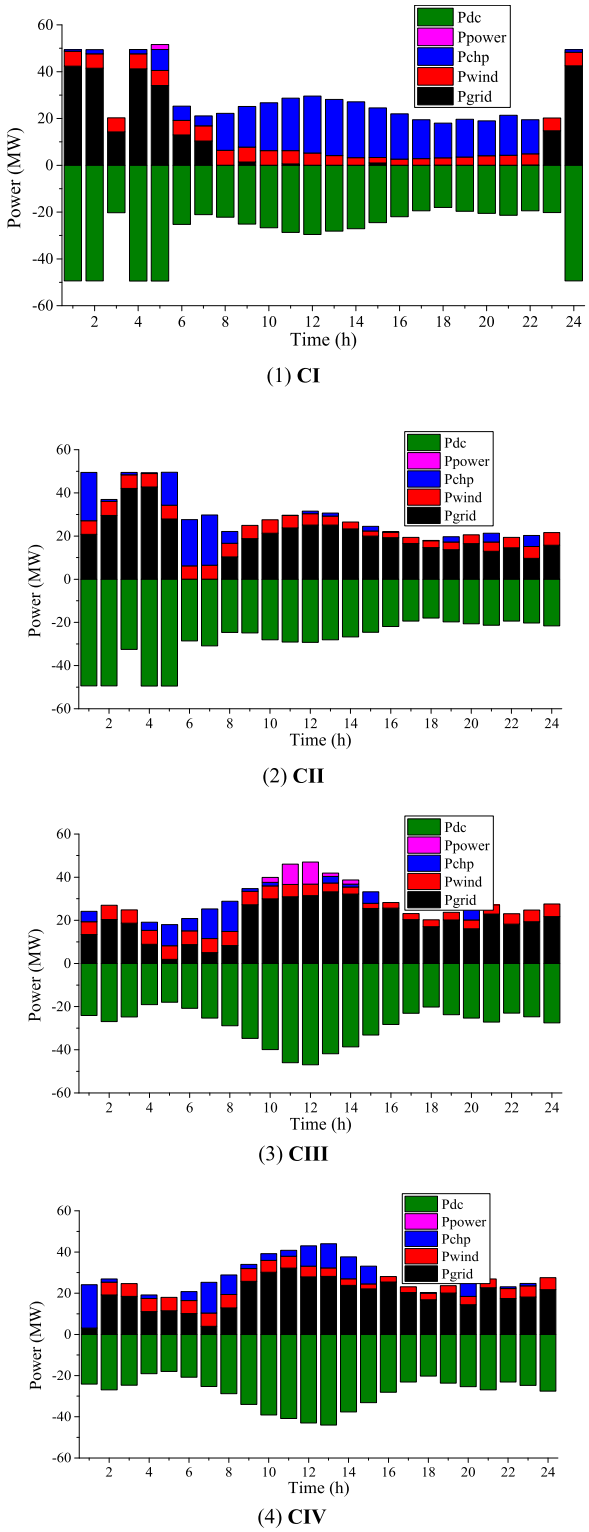

FIGURE 5. Power generation and consumption for four configurations.

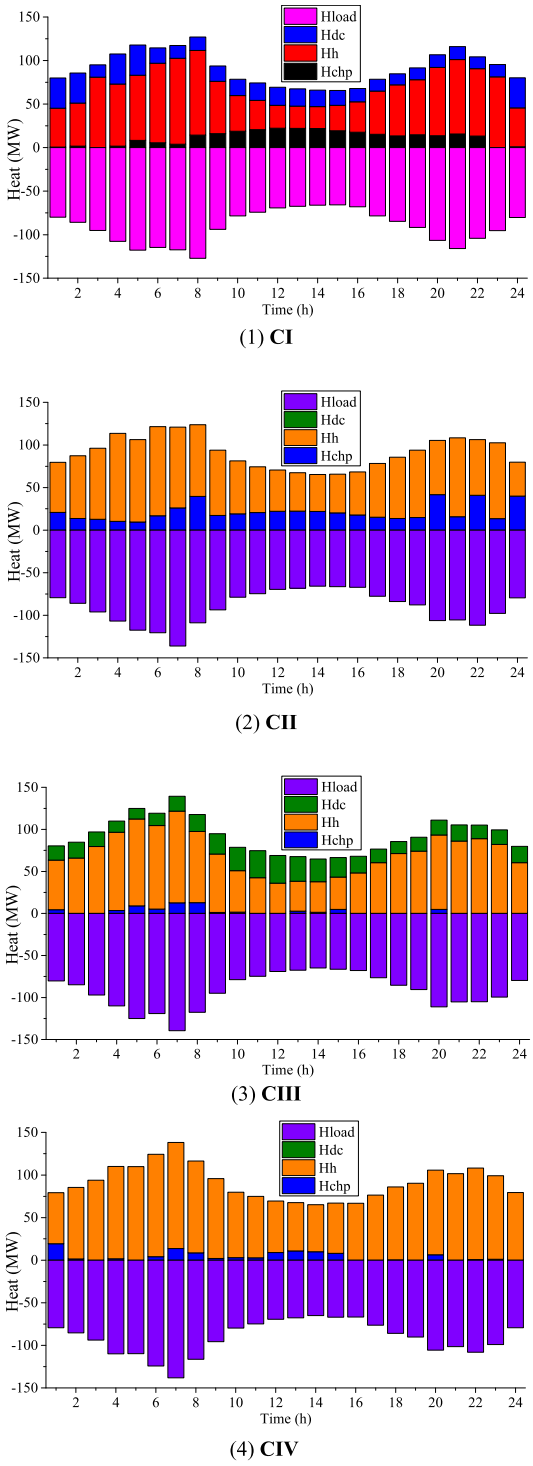

FIGURE 6. Heat production and consumption for four configurations.

when the electricity cost increases. Fig. 5(2) demonstrates the power generation and consumption in CII. Overall, the contribution of each power resources is similar to the results in CI while the biggest difference lies in that the CHP unit generates the most in CII and stays on all day. The main reason is that without WHR, most of the heat would come from HGs. This reveals that WHR process could reduce primary energy usage and the emission. Without DCWA, as shown in Fig. 5(3) and Fig. 5(4), power demands are mainly located in the daytime as stated above. Hence, on-site generation units operate at high output level during this time period, which results in producing a large portion of GHG in the meantime.

Fig. 6 shows the thermally related decision portfolios for the four configurations respectively. The histograms above the horizontal axis represent the heat generated from conventional HGs and waste heat repurposed from data center. And the thermal consumption is depicted below the horizontal axis, i.e. heating demand in the district heating area. Fig. 6(1) shows heat generation and consumption in the optimal case **CI**. As shown in Fig. 6(1), the primary heating source is the heat-only unit (63.75% of the total heat production) and then followed by the waste heat recovered from the data center (22.18% of the total heat production). The CHP unit generates 14.06% of the heat and the scheduling is made coupling with the power system. The heat resource scheduling results in **CII** is shown in Fig. 6(2). Due to the fact that no heat is recovered from the data center, the heat demand is fully served by conventional units. From Fig. 6(3) and Fig. 6(4), it can be noted that the heat served by heat-only unit dominates the most, is 96.30% and 77.85% of the total heat supply respectively. Especially in **CIV**, without WHR module, the HGs produce more heat to cover the heating demand, which results in higher economic and environmental burden to the system

The performance indexes of each configuration are shown in Table 5. It can be observed in the CSR column that the **CI** of the lowest cost. Compared with the reference case (**CIV**), 23.39% of the total cost are saved. The comparison between the cost of **CI**&**CII**, **CIII**&**CIV** shows that both DCWA and the WHR module have positive effect and advantages on reducing the operation cost. Noticing that the CSR of **CII** is little less than that of **CIII**, which illustrates that the WHR module contributes more on operation reduction in heating season. This result may vary with the heating requirements. From the WCR column, the optimal case (**CI**) is of the lowest amount of the wind curtailment compared to the remaining. The decision portfolio achieved by **CI** only abandon 2.77% of the wind power, which reveals that the proposed model could elevate the wind power usage and stimulate the wind power utilization potential of the system. Furthermore, by comparing the results in **CII** and **CIII**, both DCWA and WHR have great potential in improvement of the wind power integration. It is worth to explore the reason of wind curtailment in this study. The results show that the wind curtailment generally happens in 20:00-23:00. During this time period, it presents high thermal requirements in the system. As the power and heat production is coupled in CHP generators, to meet the much-needed heating requirement, CHP unit needs to contribute more if the heat-only unit meets the upper limit. Therefore, more power is generated simultaneously. With limited power demand, some of the wind power is rejected. From the third column, it can be observed that 11.16% of the GHG emission is reduced compared with the reference case, demonstrating a better environmental performance is achieved by the proposed model. Meanwhile, both DCWA and WHR have positive influence on emission reduction, and the latter contributes more.

Fig. 7 outlines the comparison of hourly GHG emission overall in each configuration. As shown in Fig. 7, the overall GHG emission in **CI** stays the lowest for most of time, which reveals the environmental superiority of the proposed model. The GHG emission of **CII** is slightly greater than that of **CI**. Additionally, the GHG emission of **CIII** is greater than **CII**. This could be explained that both the WHR and DCWA process have positive impacts on the emission reduction. **CIV** is of the highest emission compared to the others. It should be noted that the emission of **CI** is not at the minimum for all the hours. During the early morning (3:00-5:00 and 6:00-8:00) when the workloads re-allocate in **CI** and **CII**, the GHG emission of both configurations are greater than that of **CIII** and **CIV**. This can be explained that the system requests more power to cover the re-allocated workloads during this period in the two configurations, which leads to more GHG emissions simultaneously.

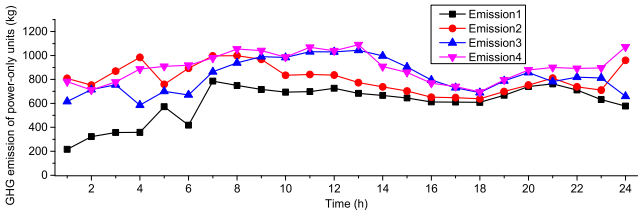

FIGURE 7. Comparison of hourly GHG emission overall in four configurations.

2) FURTHER ANALYSIS

To illustrate the impact of the key parameters on the decision portfolio for the proposed model, three further sensitivity analyses are conducted on the GHG emission tax tariffs, uncertainty analysis and the WHR conversion factors. All the technical analyses are evaluated in the optimal case.

a: GHG EMISSION TAX TARIFFS

Multiple GHG emission tax tariffs of the grid and on-site generation units are compared to demonstrate their impacts on the overall cost. As shown in Fig. 8, it can be noted that the increasing of the emission tax tariff introduces a higher operation cost. With doubled emission tax, the total operation cost becomes 10% higher than the original value. In addition, there is a negative correlation between the GHG emission tax tariff and the emission. This is because higher emission tax tariff would put a larger weight on the emission cost in the optimization objective function which leads to lower GHG emissions.

b: WIND POWER UNCERTAINTY

As mentioned above, the uncertainty level of wind power is measured by the variance of wind power forecasting error. To quantify the impact of wind power uncertainty on the decision-making and justify the effectiveness of proposed two-stage stochastic programming approach, cases with different uncertainty levels are examined and the numerical

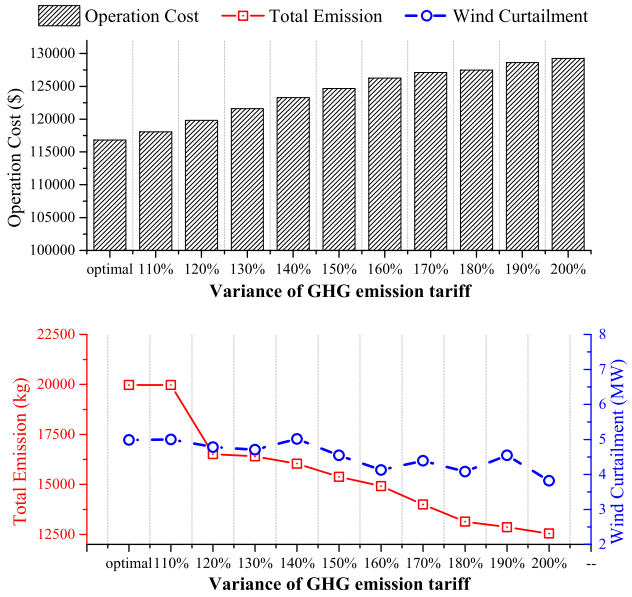

FIGURE 8. Economic and environmental impacts of GHG emission tax tariffs on the optimal configuration.

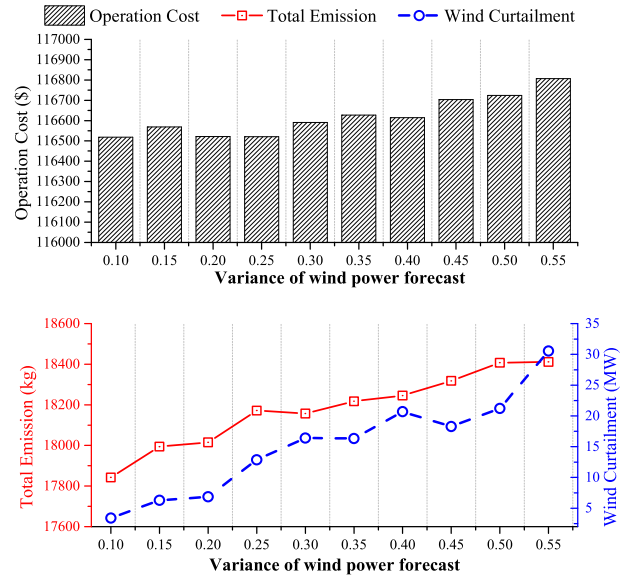

FIGURE 9. Economic and environmental impacts of the forecasting error variance of wind power on the optimal configuration.

results are reported in Fig. 9. It can be observed that the operation cost of the system, as well as total GHG emission and wind curtailment, go up as the uncertainty level of wind power increases. This could be explained by the fact that as the wind power fluctuation increases, more conventional generation units are scheduled to meet the power and heating demand and consequently more wind is curtailed. The simulation results show that reducing the wind power uncertainty (i.e. improving the wind power forecasting) can be critical to enhance the economic and environmental performance of the simulation system.

c: WHR CONVERSION FACTOR

As stated above, significant amount of wind curtailment is incurred due to the inflexibility introduced by CHP units in residential heating section [57]. To further illustrate the impact of the proposed model on improving the flexibility, especially for a CHP dominated system, the simulation system is modified to have only CHP unit which emphasizes the inflexibility of system operation due to its coupled heat and power production characteristics. In the proposed multi-energy scheduling model, the WHR module of data center can play the role of relaxing the coupled correlation between heat and power production since it can relieve the heating stress of CHP unit. The numerical simulation results are shown in Fig. 10. It can be observed that the overall operation cost decreases significantly as the WHR conversion factor increases. This can be explained that with more waste heat of data center being repurposed to meet the heating demand, CHP unit could produce less heat. Consequently, the lower bound of power production for CHP unit is reduced, which consequently reduces the inflexibility of system operation and provides more space to integrate wind power.

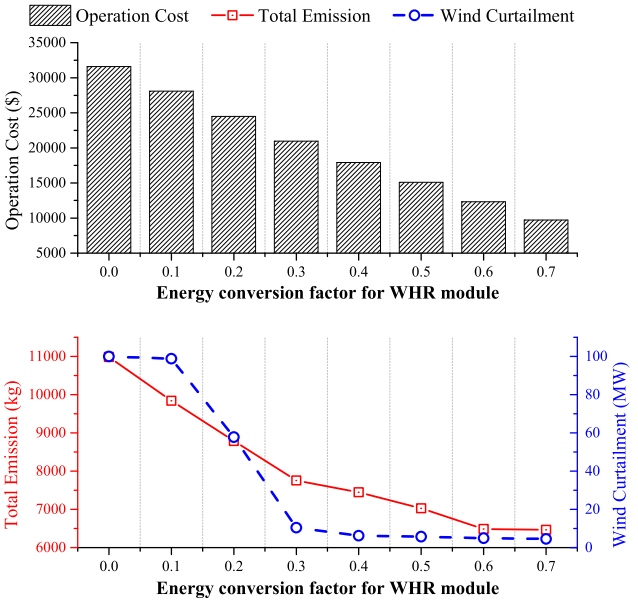

FIGURE 10. Economic and environmental effectiveness for various energy conversion factor for WHR module in the optimal configuration.

d: SCALES OF WIND POWER GENERATION

Without loss of generality, the proposed system is also analyzed with various scales of wind power generation during the heating period, which generally lasts from Nov. to Mar. of the next year. Based on the historical data [47] and the calculation method of [48], three scenarios, referring strong wind, moderate wind and light wind scenarios, are analyzed in this section. The performance indexes compared with the reference case (**CIV**) are shown in Table 6. This table outlines a comparison of the economic and environmental improvement that the different amount of wind power could achieve. This table also

TABLE 6. Indexes of various level of wind power generation during heating period compared with reference case (CIV).

	Strong	Moderate	Light
CSR (%)	58.56	23.39	13.19
GERR (%)	34.07	11.16	9.30
WCR (%)	9.15	2.77	1.81

illustrates that the operation cost decreases with the growing wind power generation. The drop-off in total GHG emission of the system could be explained that with more wind power with competitive price to be obtained, the possibility of the fossil-fueled generators utilization is reducing. What's more, the enormous amount of wind power induces randomness in the system. Dominated by the inflexibility of the system operation, large amount of the wind power would be curtailed. Moreover, this table demonstrates that with DCWA and WHR module, the economic and environmental performance could be improved, which also testified the effectiveness of the proposed model.

3) IMPACT ESTIMATION ON NORTH HEBEI

North Hebei is relatively rich in wind resources, especially in Zhangjiakou and Chengde. And the number of the wind generators is booming these years. While, transmission capability limitation of the grid in North Hebei no longer matches with requirement of rapidly growing installed wind capacity, which is the main reason inducing the curtailment [58]. Another reason of using North Hebei region as an example is that this region heavily relies on coal-fired based CHP for district heating during winter time, which not only results in higher GHG emission, but also creates inflexibility to integrate onshore wind power.

In the meantime, there constructed a large number of data centers in North Hebei [59], which benefit from the local abundant wind power resources and relatively lower rent price. Moreover, it is close to rapid developing urban areas such as Beijing and Tianjin, therefore the data centers would have number of users.

In this section, the proposed multi-energy scheduling scheme of data center is applied to North Hebei region in China to estimate how much economic and environment enhancement can be achieved.

According to surveys on large-scale data centers within NH area, the parameters are outlined in Table 7. The average power consumption of a common server per CPU in on/off state is assumed as 200 W and 100 W based on [65]. According to the research, the ratio of on-site thermal power to on-site wind power is 4:4.5 [66] After adjusting some of the data, the results of this simulation model is shown as follows.

Correspondingly, the results are shown as follows. After applying DCWA and WHR module in the system, overall North Hebei region could achieve 20.15% of the cost reduction, 35.06% of the GHG emission reduction and increase the wind usage ratio by 2%. What's more, it is worth to mention that because of the great portion of the CHP units' integration to the utility grid, the wind power contribution is relatively low. That is, big amount of the wind power is rejected. That's because with the severe heating requirements in North Hebei during winter, CHP units must operate more to meet the heating requirements of the system, which could produce more power simultaneously. With limited power load request, the wind power would be abandoned. Though the results in practice may vary from the estimated result due to the complex energy generation and workload mix, it still demonstrates great potentials in economic and environmental performance improvement of DCWA and WHR for the data center industry by adopting the proposed multi-energy scheduling scheme.

TABLE 7. Parameters of large-scale data centers in NH region.

City	Data center	Number of servers	Source
Zhangjiakou	Big Data Center, JD; Zhangbei Data Center, Ali	1,500,000	[60, 61]
Chengde	Big Data Industrial Park, Deming	400,000	[62]
Tangshan	Unicom Internet Data Center, Tangshan	180,000	[63]
	Weier Cloud Computing Center, Tangshan Iron and Steel Company	20,000	[64]

4) LIMITATIONS OF THE STUDY

The limitations of the study are provided to acknowledge the weakness of the results and to suggest the future directions of this study. As the amount of wind curtailment caused by transmission congestion in short-distance transmission is limited, the network topology and the transmission congestion are neglected in this paper, in order that the inflexibility in the system caused by the generation and operation constraints is stressed to highlight the contributions of this paper. In addition, hot water pipeline network is not considered as well. Though the research in [19] explains that data centers are usually constructed close to the district heating network and the transmission loss would be fewer, a more detailed and sophisticated thermal system with hot water pipeline network considered would be one of our future probable trends.

V. CONCLUSION

In this paper, a flexible multi-energy scheduling scheme for a data center microgrid is proposed to optimize its operation cost while facilitating more wind power integration. A two-stage stochastic programming formulation is adopted to address the uncertainties in the scheduling process. The scheduling decisions for on-site generation units, utility power procurement, shift-able batch workload allocation is optimized to meet the thermal and power demand. The proposed scheme is examined with a simulation system and numerical results demonstrate its effectiveness on reducing operation cost and promoting wind power integration.

Also, the potential impact of the proposed scheme is estimated in the North Hebei Region to demonstrate its potential effect in larger system.

REFERENCES

[1] S. Shapiro-Bengtsen. (Apr. 5, 2017). *Reducing Renewables Curtailment in China—An Air Quality Measure*. [Online]. Available: https://www.raponline.org/blog/reducing-renewables-curtailment-china-air-quality-measure/
[2] Y. Qi, W. Dong, C. Dong, and C. Huang, "Understanding institutional barriers for wind curtailment in China," *Renew. Sustain. Energy Rev.*, vol. 105, pp. 476–486, May 2019.
[3] Y. Zhang, N. Tang, Y. Niu, and X. Du, "Wind energy rejection in China: Current status, reasons and perspectives," *Renew. Sustain. Energy Rev.*, vol. 66, pp. 322–344, Dec. 2016.
[4] Y. Shu, Z. Zhang, J. Guo, and Z. L. Zhang, "Study on key factors and solution of renewable energy accommodation," *Proc. CSEE*, vol. 37, no. 1, pp. 1–8, 2017.
[5] G. Fan, N. Zhang, Z. Liang, and J. Wang, "Analysis on the 'three norths' region wind and PV power limitation," *North China Electric Technol.*, vol. 12, pp. 55–59, Aug. 2016.
[6] Z. Wu, H. Sun, and Y. Du, "A large amount of idle capacity under rapid expansion: Policy analysis on the dilemma of wind power utilization in China," *Renew. Sustain. Energy Rev.*, vol. 32, pp. 271–277, Apr. 2014.
[7] A. Jafari, T. Khalili, H. G. Ganjehlou, and A. Bidram, "Optimal integration of renewable energy sources, diesel generators, and demand response program from pollution, financial, and reliability viewpoints: A multi-objective approach," *J. Cleaner Prod.*, vol. 247, Feb. 2020, Art. no. 119100.
[8] Statista. (Apr. 2017). *Number of Data Centers Worldwide in 2015, 2017, and 2021 (in Millions)*. [Online]. Available: https://www.statista.com/statistics/500458/worldwide-datacenter-and-it-sites/
[9] *Data Center Market—Global Outlook and Forecast 2018-2023*, ResearchAndMarkets, Global, Delft, The Netherlands, 2018.
[10] A. Andrae, "Total consumer power consumption forecast," *Nordic Digit. Bus. Summit*, vol. 10, pp. 1–27, 2017.
[11] T. Chen, X. Wang, and G. B. Giannakis, "Cooling-aware energy and workload management in data centers via stochastic optimization," *IEEE J. Sel. Topics Signal Process.*, vol. 10, no. 2, pp. 402–415, Mar. 2016.
[12] L. Yu, T. Jiang, Y. Cao, and Q. Qi, "Carbon-aware energy cost minimization for distributed Internet data centers in smart microgrids," *IEEE Internet Things J.*, vol. 1, no. 3, pp. 255–264, Jun. 2014.
[13] H. Wang and Z. Ye, "Renewable energy-aware demand response for distributed data centers in smart grid," in *Proc. IEEE Green Energy Syst. Conf. (IGSEC)*, Nov. 2016, pp. 1–8.
[14] Y. Guo, Y. Gong, Y. Fang, P. P. Khargonekar, and X. Geng, "Energy and network aware workload management for sustainable data centers with thermal storage," *IEEE Trans. Parallel Distrib. Syst.*, vol. 25, no. 8, pp. 2030–2042, Aug. 2014.
[15] S. Kwon, L. Ntaimo, and N. Gautam, "Demand response in data centers: Integration of server provisioning and power procurement," *IEEE Trans. Smart Grid*, vol. 10, no. 5, pp. 4928–4938, Sep. 2019.
[16] K. Kim, F. Yang, V. M. Zavala, and A. A. Chien, "Data centers as dispatchable loads to harness stranded power," *IEEE Trans. Sustain. Energy*, vol. 8, no. 1, pp. 208–218, Jan. 2017.
[17] J. Li, Z. Bao, and Z. Li, "Modeling demand response capability by Internet data centers processing batch computing jobs," *IEEE Trans. Smart Grid*, vol. 6, no. 2, pp. 737–747, Mar. 2015.
[18] Z. Ding, Y. Cao, L. Xie, Y. Lu, and P. Wang, "Integrated stochastic energy management for data center microgrid considering waste heat recovery," *IEEE Trans. Ind. Appl.*, vol. 55, no. 3, pp. 2198–2207, May 2019.
[19] M. Wahlroos, M. Pärssinen, S. Rinne, S. Syri, and J. Manner, "Future views on waste heat utilization—Case of data centers in northern europe," *Renew. Sustain. Energy Rev.*, vol. 82, pp. 1749–1764, Feb. 2018.
[20] M. Wahlroos, M. Pärssinen, J. Manner, and S. Syri, "Utilizing data center waste heat in district heating—Impacts on energy efficiency and prospects for low-temperature district heating networks," *Energy*, vol. 140, pp. 1228–1238, Dec. 2017.
[21] J. Zachary Woodruff, P. Brenner, A. P. C. Buccellato, and D. B. Go, "Environmentally opportunistic computing: A distributed waste heat reutilization approach to energy-efficient buildings and data centers," *Energy Buildings*, vol. 69, pp. 41–50, Feb. 2014.
[22] Z. Zhou, J. Zhang, P. Liu, Z. Li, M. C. Georgiadis, and E. N. Pistikopoulos, "A two-stage stochastic programming model for the optimal design of distributed energy systems," *Appl. Energy*, vol. 103, pp. 135–144, Mar. 2013.
[23] Z. Wu, P. Zeng, X.-P. Zhang, and Q. Zhou, "A solution to the chance-constrained two-stage stochastic program for unit commitment with wind energy integration," *IEEE Trans. Power Syst.*, vol. 31, no. 6, pp. 4185–4196, Nov. 2016.
[24] C. Marino, M. A. Quddus, M. Marufuzzaman, M. Cowan, and A. E. Bednar, "A chance-constrained two-stage stochastic programming model for reliable microgrid operations under power demand uncertainty," *Sustain. Energy, Grids Netw.*, vol. 13, pp. 66–77, Mar. 2018.
[25] Q. Wang, Y. Guan, and J. Wang, "A chance-constrained two-stage stochastic program for unit commitment with uncertain wind power output," *IEEE Trans. Power Syst.*, vol. 27, no. 1, pp. 206–215, Feb. 2012.
[26] D. Wang, J. Qiu, L. Reedman, K. Meng, and L. L. Lai, "Two-stage energy management for networked microgrids with high renewable penetration," *Appl. Energy*, vol. 226, pp. 39–48, Sep. 2018.
[27] L. Yu, T. Jiang, and Y. Zou, "Distributed real-time energy management in data center microgrids," *IEEE Trans. Smart Grid*, vol. 9, no. 4, pp. 3748–3762, Jul. 2018.
[28] W. Qi and J. Li, "Towards optimal coordinated operation of distributed Internet data center microgrids," in *Proc. IEEE Power Energy Soc. Gen. Meeting (PESGM)*, Jul. 2016, pp. 1–5.
[29] W. Qi, J. Li, Y. Liu, and C. Liu, "Planning of distributed Internet data center microgrids," *IEEE Trans. Smart Grid*, vol. 10, no. 1, pp. 762–771, Jan. 2019.
[30] A. Ali and O. Ozkasap, "Price/cooling aware and delay sensitive scheduling in geographically distributed data centers," in *Proc. NOMS-IEEE/IFIP Netw. Operations Manage. Symp.*, Apr. 2016, pp. 1025–1030.
[31] Z. Liu, Y. Chen, C. Bash, A. Wierman, D. Gmach, Z. Wang, M. Marwah, and C. Hyser, "Renewable and cooling aware workload management for sustainable data centers," *ACM SIGMETRICS Perform. Eval. Rev.*, vol. 40, no. 1, pp. 175–186, Jun. 2012.
[32] B. Zhao, A. J. Conejo, and R. Sioshansi, "Unit commitment under gas-supply uncertainty and gas-price variability," *IEEE Trans. Power Syst.*, vol. 32, no. 3, pp. 2394–2405, May 2017.
[33] S.-R. Lim, Y. R. Kim, S. H. Woo, D. Park, and J. M. Park, "System optimization for eco-design by using monetization of environmental impacts: A strategy to convert bi-objective to single-objective problems," *J. Cleaner Prod.*, vol. 39, pp. 303–311, Jan. 2013.
[34] M. J. Salehpour and S. M. M. Tafreshi, "Optimal bidding strategy for a smart microgrid in day-ahead electricity market with demand response programs considering uncertainties," in *Proc. Smart Grid Conf. (SGC)*, Dec. 2017.
[35] Z. Ding and W.-J. Lee, "A stochastic microgrid operation scheme to balance between system reliability and greenhouse gas emission," *IEEE Trans. Ind. Appl.*, vol. 52, no. 2, pp. 1157–1166, Mar./Apr. 2016.
[36] A. P. R. A. Shapiro, *Stochastic Programming*. Amsterdam, The Netherlands: Elsevier, 2003.
[37] Z. Li, C. Zang, P. Zeng, H. Yu, and H. Li, "Two-stage stochastic programming based model predictive control strategy for microgrid energy management under uncertainties," in *Proc. Int. Conf. Probabilistic Methods Appl. Power Syst. (PMAPS)*, Oct. 2016, pp. 1–6.
[38] N. Good, E. A. Martínez Ceseña, L. Zhang, and P. Mancarella, "Techno-economic and business case assessment of low carbon technologies in distributed multi-energy systems," *Appl. Energy*, vol. 167, pp. 158–172, Apr. 2016.
[39] J. Aghaei and M.-I. Alizadeh, "Multi-objective self-scheduling of CHP (combined heat and power)-based microgrids considering demand response programs and ESSs (energy storage systems)," *Energy*, vol. 55, pp. 1044–1054, Jun. 2013.
[40] A. Ramos, *Stochastic Optimization*. Norwell, MA, USA: Kluwer, 2003.
[41] Ç. U. Güler, M. Ermis, and M. Ermis, "A deterministic model to the two-stage stochastic programming of disaster-relief supply chain transportation and distribution planning," presented at the World Congr. Eng. (WCE), London, U.K., 2014.
[42] P. Wang, L. Xie, Y. Lu, and Z. Ding, "Day-ahead emission-aware resource planning for data center considering energy storage and batch workloads," in *Proc. IEEE Conf. Energy Internet Energy Syst. Integr. (EI2)*, Piscataway, NJ, USA, Nov. 2017, p. 6.
[43] A. R. C. Belady, J. Pfleuger, and T. Cader, "Green grid data center power efficiency metrics: PUE and DCIE," Green Grid, Beaverton, OR, USA, Tech. Rep., 2008.

[44] L. Yu, T. Jiang, S. Member, Y. Cao, and S. Member, "Risk-constrained operation for Internet data centers in deregulated electricity markets," *IEEE Trans. Parallel Distrib. Syst.*, vol. 25, no. 5, pp. 1306–1316, May 2014.
[45] D. O. Energy, "Waste heat recovery technology assessment," in *The Quadrennial Technology Review (QTR)*. Washington, DC, USA: Industry and Manufacturing, 2015, ch. 8.
[46] ORACLE. (2010). *Batch Workloads*. [Online]. Available: https://docs.oracle.com/cd/E19112-01/ctr.mgr11/816-7751/6mdo2so0h/index.html
[47] (2018). *Weather History Download Basel*. [Online]. Available: https://www.meteoblue.com/en/weather/archive/export/basel_switzerland_2661604
[48] H. Ren and W. Gao, "A MILP model for integrated plan and evaluation of distributed energy systems," *Appl. Energy*, vol. 87, no. 3, pp. 1001–1014, Mar. 2010.
[49] R. Renaldi, A. Kiprakis, and D. Friedrich, "An integrated framework for the optimal design of low carbon residential heating systems," *Appl. Energy*, vol. 186, pp. 520–529, 2016.
[50] (2018). *Overview of Greenhouse Gases*. [Online]. Available: https://www.epa.gov/ghgemissions/overview-greenhouse-gases
[51] *Fuel Mix Disclosure Data Table*, Dept. Business, Energy Ind. Strategy Res. Anal., London, U.K., Aug. 2018.
[52] M. Nemati, M. Braun, and S. Tenbohlen, "Optimization of unit commitment and economic dispatch in microgrids based on genetic algorithm and mixed integer linear programming," *Appl. Energy*, vol. 210, pp. 944–963, Jan. 2018.
[53] PJM. *Real-Time Hourly LMPs*. Accessed: Nov. 28, 2018. [Online]. Available: https://dataminer2.pjm.com/feed/rt_hrl_lmps
[54] Z. Ding, L. Xie, Y. Lu, P. Wang, and S. Xia, "Emission-aware stochastic resource planning scheme for data center microgrid considering batch workload scheduling and risk management," *IEEE Trans. Ind. Appl.*, vol. 54, no. 6, pp. 5599–5608, Nov. 2018.
[55] Data Center Knowledge. (Mar. 16, 2017). *Google Data Center FAQ*. [Online]. Available: https://www.datacenterknowledge.com/archives/2017/03/16/google-data-center-faq
[56] P. Jochem, M. Schönfelder, and W. Fichtner, "An efficient two-stage algorithm for decentralized scheduling of micro-CHP units," *Eur. J. Oper. Res.*, vol. 245, no. 3, pp. 862–874, Sep. 2015.
[57] G.-L. Luo, Y.-L. Li, W.-J. Tang, and X. Wei, "Wind curtailment of China's wind power operation: Evolution, causes and solutions," *Renew. Sustain. Energy Rev.*, vol. 53, pp. 1190–1201, Jan. 2016.
[58] X. Guo, D. Ren, and C. Li, "Study on the problem of wind power curtailment in Beijing-Tianjin-Hebei based on risk-return," *Energy Sour., A, Recovery, Utilization, Environ. Effects*, vol. 1, pp. 1–16, May 2019.
[59] B. Stoller. (Nov. 26, 2018). *Why GDS Thinks It'll Go on Winning in the Chinese Data Center Market*. [Online]. Available: https://www.datacenterknowledge.com/investing/why-gds-thinks-it-ll-go-winning-chinese-data-center-market
[60] JD.Com. *Data Science Lab*. Accessed: Feb. 13, 2020. [Online]. Available: https://datascience.jd.com/
[61] Alibaba.Com. *Alibaba Cloud*. Accessed: Feb. 13, 2020. [Online]. Available: https://www.alibabacloud.com/
[62] BeijingJournal. (Dec. 12, 2016). *Chengde Will Build the Largest Green Data Center Around Beijing*. [Online]. Available: http://tech.idcquan.com/104529.shtml
[63] IDC-China. (2016). *The Chengde Municipal Government Will Visit Fay News to Work Together to Build a Cloud Computing Data Center Project*. [Online]. Available: http://cloud.idcquan.com/yzx/91758.shtml
[64] (2013). *Weier Cloud Computing Center, Tangshan Iron and Steel Company*. [Online]. Available: http://dian.idcquan.com/item.php?act=detail&id=1509
[65] A. Fernández-Montes, D. Fernández-Cerero, L. González-Abril, J. A. Álvarez-García, and J. A. Ortega, "Energy wasting at Internet data centers due to fear," *Pattern Recognit. Lett.*, vol. 67, pp. 59–65, Dec. 2015.
[66] *2017 Annual Inspection Comprehensive Supervision Report*, SGJEPC Ltd., North Jibei, 2018.

PENG WANG received the B.S., M.S., and Ph.D. degrees from North China Electric Power University, in 1994, 1997, and 2002, respectively. He used to be the Director of the Department of Power Regulatory, China, for a long time. He is currently a Professor with the School of Electrical and Electronics Engineering, North China Electric Power University. His research areas include power market design and regulation, energy policy, and carbon market.

YUJIE CAO (Student Member, IEEE) received the B.S. degree in electrical engineering from North China Electric Power University, Beijing, China, in 2017, where she is currently pursuing the M.S. degree in electric power system and automation with the School of Electrical and Electronics Engineering. Her areas of interest include power system operation, data centers, and power markets.

ZHAOHAO DING (Member, IEEE) received the B.S. degree in electrical engineering and the B.A. degree in finance from Shandong University, Jinan, China, in 2010, and the Ph.D. degree in electrical engineering from The University of Texas at Arlington, in 2015. He is currently an Assistant Professor with North China Electric Power University and a Research Member of the Academy of Modern Electric Power Research. His areas of interest include power system planning and operation, power markets, and stochastic optimization.